Spin-orbit-interaction-induced generation of optical vortices in multihelicoidal fibers

C. N. Alexeyev,[1,*] A. N. Alexeyev,[2] B. P. Lapin,[1] G. Milione,[3,4,5] and M. A. Yavorsky[1]

[1]*Taurida National V. I. Vernadsky University, Vernadsky Prospekt, 4, Simferopol, 95007, Crimea, Ukraine*

[2]*National Academy of Sciences of Ukraine, Karadag Nature Reserve, 24 Nauki strasse, Kurortnoe, Feodosia, 98188, Crimea, Ukraine*

[3]*Institute for Ultrafast Spectroscopy and Lasers, Physics Department, City College of New York of the City University of New York, 160 Convent Avenue, New York, New York 10031, USA*

[4]*Graduate Center of New York of the City University of New York, 365 Fifth Avenue, New York, New York 10016, USA*

[5]*New York State Center for Complex Light, 160 Convent Avenue, New York, New York 10031, USA*

(Received 6 September 2013; revised manuscript received 8 November 2013; published 5 December 2013)

We have studied the effect of the spin-orbit interaction on generation and conversion of optical vortices in multihelicoidal fibers, that is, the fibers possessing a multihelical refractive index profile. On the basis of a fully analytical approach we have obtained the spectra of coupled modes and their structure. Specifically, we have established selection rules, under which the spin-orbit interaction mediates the conversion of optical vortices into vortices with the topological charge changed by $\pm(\ell \pm 2)$, ℓ being the number of helical branches in refractive index distribution. Also, we have shown that the spin-orbit interaction can lead to generation of radially and azimuthally polarized TE and TM modes from optical vortices. We have also demonstrated that if such generation is mediated by a scalar-type perturbation of the fiber's form, it is possible only for weakly deformed fibers. For strongly deformed fibers such perturbation can result only in generation of vortices with zero total angular momentum. Additionally, we have studied the possibility of polarization control over the orbital angular momentum of the generated state in such a system.

DOI: 10.1103/PhysRevA.88.063814 PACS number(s): 42.25.Bs, 42.81.Qb, 42.81.Bm

I. INTRODUCTION

A multihelicoidal fiber (MHF) is an optical fiber possessing a multihelical refractive index profile as shown in Fig. 1. The refractive index distribution of a MHF has ℓ helical branches and possesses the ℓ-fold rotational symmetry. Recent theoretical studies of such fibers have revealed their ability to change the topological charge of incoming beams in both transmitted [1–4] and reflected fields [5]. Certain types of photonic crystal fibers (PCFs) also belong to such a class of optical fibers [6]. These works have shown that in a certain spectral range the spiraling lattice imparts its "imprinted" charge, which coincides with the order of symmetry ℓ, to the incoming field with a well-defined topological charge changing it by $\pm\ell$ units. This ability to control the topological charge of the output beam and its orbital angular momentum (OAM) could be useful in information applications of OAM carrying beams both in free space [7–10] and, especially, in optical fibers [11,12].

However, there are sharp discrepancies between scalar and vector approximations to the analysis of MHFs. The above-mentioned analysis has been limited to the scalar approximation, which makes it impossible to reveal all the variety of intermodal transitions in MHFs. Meticulous studies beyond the scalar approximation, carried out by Xu and co-workers [13,14], demonstrate the existence of a different class of mode transitions. In those transitions the topological index of the generated field can be changed by $\ell \pm 2$ units, rather than by the "charge" ℓ of the lattice, as the scalar-approximation theory predicts. As has been indicated, such mode transformations also involve flipping of the circular polarization of the incoming field. All such effects are impossible to uncover within the frameworks of the scalar approximation, which implies conservation of the spin state of the field in the process of mode transformation.

The reported change of spin accompanied by the change of the OAM state gives evidence that the transformation is mediated by the spin-orbit interaction (SOI). However, the approach, used in those inspiring works and suggested in Refs. [15,16], has not allowed the authors to establish the dynamical reason of such a novel effect connected with the SOI. As a consequence, the authors have not emphasized the importance of spin transformations during mode transitions concealing such information in a simple angular momentum (AM) selection rule established in Eq. (2) of Ref. [14]. Meanwhile, the type of interaction, which mediates the mode transition, determines not only its main characteristics and the spatial scale of mode transformation. In some cases the type of mode transformation is determined not only by formal selection rules but also by the proximity of other points of resonant mode transitions. It turns out that for ill-resolved in wavelength mode transition points the mutual influence of neighboring resonant transitions may drastically change the type of such transitions. In this way, neglecting the factor of proximity of such resonant points connected with generation of the TE and TM modes the authors made some incorrect statements on the possibility of their generation in MHFs. Although this fact does not diminish the significance and scientific quality of the mentioned papers, it is desirable to analyze in detail the role of the SOI on mode transformations in MHFs.

In this paper we provide an analytical treatment of resonance mode transitions in MHFs and demonstrate the effect of the SOI on the conversion of optical vortices (OVs) in MHFs. We construct the SOI Hamiltonian and establish dynamical

*Corresponding author: c.alexeyev@yandex.ua

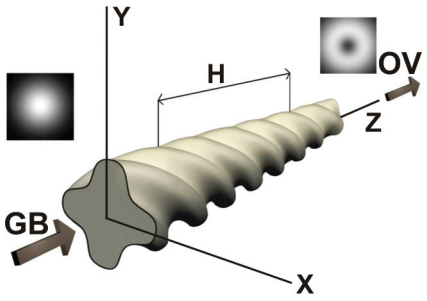

FIG. 1. (Color online) The model of an $\ell = 4$ MHF. Note that the pitch H is 4 times greater than the minimal distance, at which the refractive index is restored. Shown schematically is the generation of an OV from $m = 0$ Gaussian beam (intensity distribution is given).

and kinematical selection rules for possible resonance mode transitions in such fibers. We also obtain the values of the corresponding coupling coefficients and show that for the SOI-induced transitions a narrow-band generation of the TE and TM modes from the input OV beams is possible. For the transitions induced by a strong scalar perturbation the only possible type is a broadband generation of OVs.

II. BASIC EQUATIONS AND THE SPIN-ORBIT-INTERACTION HAMILTONIAN

Chiral fiber gratings have long been under consideration in fiber optics [14–18], although the majority of works have been devoted to the study of circular birefringence in them [17,19–27]. Only quite recently the focus of attention has somewhat shifted to the study of higher-order mode propagation in such optical systems, including nonlinear and PCFs [28]. The refractive index distribution in such a MHF has the form [29]

$$n^2(r,\varphi) \approx \tilde{n}^2 - n_{\rm co}^2 \Phi(r) \cos \ell(\varphi - qz) \equiv \tilde{n}^2 - \nu^2, \qquad (1)$$

where $\tilde{n}^2 = n_{\rm co}^2[1 - 2\Delta f(r)]$ is the refractive index of the unperturbed ideal fiber, $\Phi(r) = 2\Delta\delta r f'$, Δ is the height of the profile f, $\delta \ll 1$ is the dimensionless parameter of the cross section's deformation, $n_{\rm co}$ is the core's refractive index, and $q = 2\pi/H$, H being the pitch of the lattice. The cylindrical-polar coordinates (r,φ,z) are introduced in the standard way. The electric field in optical fibers satisfies the so-called vector wave equation [30], which can be reduced for long-period fiber gratings to the equation in the transverse electric field $\mathbf{E}_t$:

$$(\nabla^2 + k^2 n^2)\mathbf{E}_t = -\nabla_t(\mathbf{E}_t \cdot \nabla_t \ln n^2), \qquad (2)$$

where k is the wave number in vacuum and $\nabla_t = (\partial/\partial x, \partial/\partial y)$. Without its right-hand side this equation turns into the scalar wave equation. As is known, the right-hand side of Eq. (2) comprises the effect of the SOI in optical fibers [31]. The notion of the SOI for photons has been introduced by Zel'dovich *et al.* [32]. Basically, it describes the influence of spin (polarization) properties of an electromagnetic wave on the spatial (orbital) characteristics of its energy propagation. In optical fibers the SOI is also manifested through the difference in the propagation constants of certain modes with the same orbital number m (at $m \geqslant 2$) and opposite circular polarizations. This basic interaction is the reason of a number of optical phenomena, such as the optical Magnus effect, etc. [33,34]. The SOI plays an important role in forming the mode structure of weakly guiding fibers, where the wave properties of light are essential.

We will restrict our further considerations to the case of weakly guiding fibers ($\Delta \ll 1$). For such fibers the gradient SOI term on the right of Eq. (2) is additive since $\ln n^2 \approx \ln \tilde{n}^2 - (\nu^2/n_{\rm co}^2)$. In this way, the SOI is divided into two different parts. The first part depends on the refractive index distribution of the ideal fiber $\tilde{n}$ and stands for a "background" SOI. The second part involves the correction to $\tilde{n}$, which makes the fiber ℓ-fold rotational symmetric. One can expect that these two parts of the SOI would manifest themselves separately. The main feature of Eq. (2) is its translational noninvariance in z. The standard procedure of regaining the desired invariance in z comprises an effective transition to the corotating frame. To this end one has to recast Eq. (2) in a matrix form in the basis of circular polarizations, in which $\mathbf{E}_t \sim |\Psi\rangle = \mathrm{col}(E_+, E_-)$ and $E_\pm = \frac{1}{\sqrt{2}}(E_x \mp i E_y)$ [29]. Then in the obtained equation, which has the form $\hat{H}|\Psi\rangle = 0$, where $\hat{H}$ is a certain matrix operator, it is necessary to make the following transformations:

$$\begin{aligned} \hat{H} &\to C\hat{H}C^{-1} \equiv \hat{\tilde{H}}, \\ |\Psi\rangle &\to C|\Psi\rangle \equiv |\tilde{\Psi}\rangle = \mathrm{col}(\tilde{E}_+, \tilde{E}_-), \end{aligned} \qquad (3)$$

where $C = \mathrm{diag}(e^{iqz}, e^{-iqz})$. Having carried out these transformations one should pass to the new variables: $\tilde{r} = r$, $\tilde{z} = z$, $\tilde{\varphi} = \varphi - qz$. The obtained equation turns out to be translational invariant with respect to $\tilde{z}$, which enables one to make the standard substitution: $\tilde{\mathbf{E}}_t(\tilde{r},\tilde{\varphi},\tilde{z}) = \tilde{\mathbf{e}}_t(\tilde{r},\tilde{\varphi})\exp(i\beta\tilde{z})$, where β is the propagation constant. The resulting equation in $|\tilde{\psi}\rangle = \mathrm{col}(\tilde{e}_+, \tilde{e}_-)$ reads as

$$\left[\nabla_t^2 + k^2 n^2 - (\beta - q\hat{J}_z)^2 + \hat{H}_{\rm so} + \hat{V}_{\rm so}\right]|\tilde{\psi}\rangle = 0, \qquad (4)$$

where $\hat{J}_z = \hat{l}_z + \hat{\tau}_3$ is the total AM operator, $\hat{l}_z = -i\partial/\partial\tilde{\varphi}$, and $\hat{\tau}_i$ is the Pauli matrix. Also in Eq. (4) $\hat{H}_{\rm so}$ is the operator of the SOI in ideal fibers, which reads as [31]

$$\begin{aligned} \hat{H}_{\rm so} = {} & (2\psi + \tilde{r}\psi' + \tilde{r}\psi\nabla_{\tilde{r}})\hat{\tau}_0 + \psi\hat{\tau}_3\hat{l}_z \\ & + \begin{pmatrix} 0 & \exp(-2i\tilde{\varphi})\hat{a}_+ \\ \exp(2i\tilde{\varphi})\,\hat{a}_- & 0 \end{pmatrix}, \end{aligned} \qquad (5)$$

where $\hat{a}_\pm = \tilde{r}\psi\nabla_{\tilde{r}} + \tilde{r}\psi' \pm \psi\hat{l}_z$ and $\psi = \Delta f'/\tilde{r}$. Here and in the following the primes stand for the derivatives with respect to $\tilde{r}$. The operator $\hat{V}_{\rm so}$ of the SOI induced by the deformation of the cross section is given by

$$\hat{V}_{\rm so} = \frac{1}{2}\left[\hat{\Sigma}_0\hat{\tau}_0 + \hat{\Sigma}_3\hat{\tau}_3 - \begin{pmatrix} 0 & \exp(-2i\tilde{\varphi})\,\hat{b}_- \\ \exp(2i\tilde{\varphi})\,\hat{b}_+ & 0 \end{pmatrix}\right], \qquad (6)$$

where

$$\begin{aligned} \hat{b}_\mp = {} & \cos\ell\tilde{\varphi}\left[\Phi'' - \frac{1}{\tilde{r}}\Phi' + \frac{\ell^2}{\tilde{r}^2}\Phi + \Phi'\left(\nabla_{\tilde{r}} \mp \frac{i}{\tilde{r}}\nabla_{\tilde{\varphi}}\right)\right] \\ & \pm \frac{i\ell}{\tilde{r}^2}\sin\ell\tilde{\varphi}[2\tilde{r}\Phi' - 2\Phi + \Phi(\tilde{r}\nabla_{\tilde{r}} \mp i\nabla_{\tilde{\varphi}})], \\ \hat{\Sigma}_0 = {} & \frac{\ell\Phi}{\tilde{r}^2}\sin\ell\tilde{\varphi}\nabla_{\tilde{\varphi}} - \Phi'\cos\ell\tilde{\varphi}\nabla_{\tilde{r}}, \\ \hat{\Sigma}_3 = {} & \frac{i}{\tilde{r}}[\ell\Phi\sin\ell\tilde{\varphi}\nabla_{\tilde{r}} + \cos\ell\tilde{\varphi}\Phi'\nabla_{\tilde{\varphi}}]. \end{aligned}$$

III. PERTURBATION THEORY AND RESONANCE COUPLING

Equation (4) represents a special type of eigenvalue problem, in which it is convenient to choose $\hat{H}_0 = \nabla_t^2 + k^2\tilde{n}^2 - (\beta - q\hat{J}_z)^2$ for the unperturbed zero-approximation operator. Then from the zero-approximation eigenvalue equation $\hat{H}_0(\bar{\beta})|\tilde{\psi}_0\rangle = \bar{\beta}^2|\tilde{\psi}_0\rangle$, where $|\tilde{\psi}_0\rangle$ is the zero-approximation eigenfunction (mode), one can obtain for $\bar{\beta}$ [1,2]

$$\bar{\beta}_m = \tilde{\beta}_m + Jq, \tag{7}$$

where $J = m + \sigma$ is the index of the total AM of the eigenfunction, $\tilde{\beta}_m$ is the scalar propagation constant of the corresponding ideal-fiber mode [30], and $m = 0,1,2\cdots$ is its azimuthal index (here and throughout we omit the radial number). In the weak guidance limit it is convenient to choose the eigenfunctions $|\tilde{\psi}_0\rangle$ in the form of OVs $|\sigma,m\rangle$ [31,35], which in the basis of linear polarizations $|e\rangle = \mathrm{col}(e_x,e_y)$ can be represented as

$$|\sigma,m\rangle = \begin{pmatrix} 1 \\ i\sigma \end{pmatrix} \exp(im\tilde{\varphi})F_m(\tilde{r}), \tag{8}$$

where $\sigma = \pm 1$ determines the sense of circular polarization, m specifies the topological charge and the radial function F_m satisfies the standard equation [30]. Note that the same vectors in the basis of circular polarizations $|\psi\rangle = \mathrm{col}(e_+,e_-)$ will have a different form, for example, $\mathrm{col}(1,0)\exp(im\tilde{\varphi})F_m(\tilde{r})$ for the state $|1,m\rangle$. Generally, the spectra [Eq. (7)] are not degenerate; however, at certain q the spectral curves may intersect. The position of such points of accidental degeneracy, where the spectral curves for $|\sigma,m\rangle$ and $|\sigma',m'\rangle$ zero-approximation eigenfunctions intersect, is determined by

$$q_0 = \frac{\tilde{\beta}_{m'} - \tilde{\beta}_m}{J - J'}, \quad \bar{\beta}_m(q_0) = \frac{J\tilde{\beta}_{m'} - J'\tilde{\beta}_m}{J - J'}, \tag{9}$$

where the first equation represents the kinematical resonance condition for modes with OAM, first introduced in [1]. The examples of such intersections are given in Fig. 2(a). Note that here and throughout the requirement $q_0 > 0$ imposes an additional restriction on the type of possible mode coupling.

Near such points the hybridization of the corresponding zero-approximation modes is possible. However, whether the coupling between the modes $|i\rangle$ and $|j\rangle$ does take place is dictated by the dynamical condition, which reads as $V_{ij} \equiv \langle i|\hat{V}|j\rangle \neq 0$, where the perturbation operator is $\hat{V} = \hat{H}_{\mathrm{so}} + \hat{V}_{\mathrm{so}} - k^2\nu^2$. The scalar product here is defined in the standard way:

$$\langle\Phi|\Psi\rangle = \iint_S (\,\Phi_+^* \quad \Phi_-^*\,) \begin{pmatrix} \Psi_+ \\ \Psi_- \end{pmatrix} dS, \tag{10}$$

where S is the total transverse cross section of the fiber. The condition $V_{ij} \neq 0$ provides dynamical selection rules for possible transitions. As has been shown [3], the scalar-type perturbation $k^2\nu^2$ enables the coupling between the states with

$$|m - m'| = \ell, \ \sigma = \sigma', \tag{11}$$

which presents the selection rule for the scalar-perturbation-induced transitions. Note that although Eq. (11) can also be represented as $|J - J'| = \ell$, the previous form is more informative since it comprises information on the spin and orbital indices separately. Equation (11) explicitly indicates that the coupling is induced by the scalar-type operator term, which does not imply spin changes, and does not comprise the SOI. It should be noted that the first condition in Eq. (11) allows transitions with both the raising and the lowering of the orbital index by ℓ for a lattice with the same chirality [see Fig. 2(a)]. This is possible due to the fact that the scalar-type perturbation in this case comprises the factor $\cos\ell\varphi \sim \exp(i\ell\varphi) + \exp(-i\ell\varphi)$, which makes nonzero the scalar product for the state vectors with $|\Delta m| = \ell$.

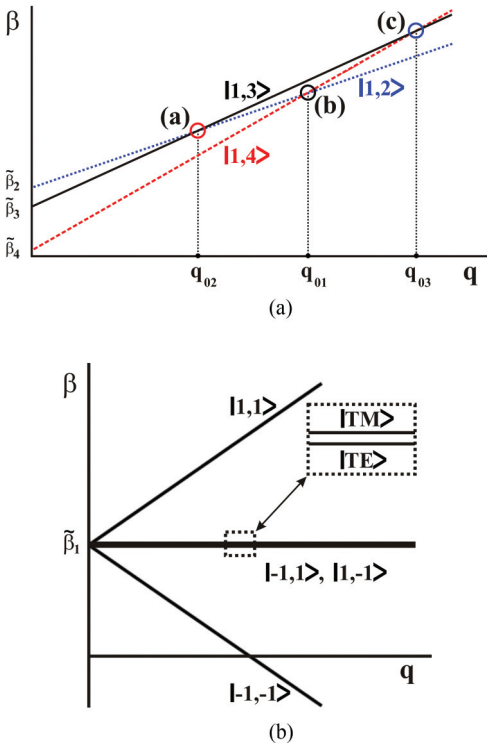

FIG. 2. (Color online) Plots of zero-approximation spectral curves and resonance points. (a) illustrates the statement that the scalar-perturbation term enables transitions with both the raising and the lowering of the orbital index of the incident mode ($|1,3\rangle$, black solid line) by ℓ (here $\ell = 1$, which stands for a helical-core fiber). In the point (a) it can be converted into the mode $|1,2\rangle$ (blue dotted line) with the lowering of the orbital index, whereas in the point (c) it can be converted into the mode $|1,4\rangle$ (red dashed line) with the raising of the orbital index. In the point (b), although the resonance conditions are met, no conversion between the modes $|1,2\rangle$ and $|1,4\rangle$ takes place since the dynamical selection rule [Eq. (11)] is not satisfied. (b) shows the spectral curves for the mode family $|m| = 1$. Note a double degeneracy of $J = 0$ curves for $|1,-1\rangle$ and $|-1,1\rangle$ OVs. Inset shows degeneracy lifting due to the SOI with the forming of the $|\mathrm{TE}\rangle$ and $|\mathrm{TM}\rangle$ modes spectral curves.

Consider now the effect of the standard ideal-fiber SOI term $\hat{H}_{\mathrm{so}}$ on the mode coupling. As is evident [31], this interaction couples only the fields $|\sigma,m\rangle$ with $\Delta J = 0$. Using (9) one can show that this entails $q_0 = \infty$; that is, the corresponding spectral curves do not intersect. Exceptions to this rule are the fields $|1,-1\rangle$ and $|-1,1\rangle$, whose spectral curves coincide [see Fig. 2(b)]. In this case the SOI lifts the degeneracy by splitting these lines (see inset) and forms the standard $|\mathrm{TE}\rangle$ and $|\mathrm{TM}\rangle$ modes. Although this part of the SOI does not couple the

modes $|\sigma,m\rangle$ other than in the above given sense, it makes the mode coupling induced by other perturbation terms more versatile, as will be shown further.

The most interesting part of the SOI Hamiltonian is the $\hat{V}_{\rm so}$ term, which originates due to the cross influence of the scalar-type perturbation term and the gradient term on the right of Eq. (2) and describes the SOI induced by the special rotational symmetry of the lattice in question. As can be easily shown, this operator couples the states $|\sigma,m\rangle$ and $|\sigma',m'\rangle$ in the case

$$m' - m - 2\sigma = \mp\ell, \quad \sigma = -\sigma', \tag{12}$$

which presents the dynamical selection rule for coupling by the second part of the SOI operator. As earlier, Eq. (12) can be represented as $|J - J'| = \ell$; however, for the same reason we prefer the expanded form of this selection rule. Note that here for definiteness we assume that the order of indices in the matrix element is as follows: $\langle\sigma,m|\hat{V}_{\rm so}|\sigma',m'\rangle$. The corresponding q, at which such a coupling takes place, is

$$q_0 = \pm(\tilde{\beta}_{m'} - \tilde{\beta}_m)/\ell, \tag{13}$$

which conveys the kinematical selection rule. The signs in Eqs. (12) and (13) should be chosen correspondingly, which guarantees the existence of two possible types of transitions connected with the raising and the lowering of topological charge by $\ell \pm 2$ units. Note that while calculating the resonance pitch we take into consideration that $\tilde{\beta}_{m'} > \tilde{\beta}_m$ if $m > m'$. Once again, the increment of the AM in such a transition is $|J - J'| = \ell$, as in the case of the scalar-perturbation term [see Eq. (11)].

IV. SPIN-ORBIT-INTERACTION-INDUCED GENERATION OF OPTICAL VORTICES

As is known, to establish the structure of hybrid modes near the points of accidental degeneracy one has to build the matrix G of the total Hamiltonian over the basis of such eigenvectors of $\hat{H}_0$, whose spectral curves intersect [1–3]. In the simplest case of intersection of two curves, which correspond to zero-approximation eigenvectors $|\sigma,m\rangle$ and $|\sigma',m'\rangle$, that matrix has the form

$$G(m,m') = \begin{pmatrix} \tilde{\beta}_m^2 - (\beta - Jq)^2 & 2\tilde{\beta}_0 Q \\ 2\tilde{\beta}_0 Q & \tilde{\beta}_{m'}^2 - (\beta - J'q)^2 \end{pmatrix}, \tag{14}$$

where Q is the corresponding coupling integral:

$$Q = \frac{1}{2\tilde{\beta}_0}\langle\sigma,m|\hat{V}|\sigma',m'\rangle. \tag{15}$$

It is implied here that the solution $\mathbf{x} = \mathrm{col}(x_1,x_2)$ of the eigenvector equation $G(m,m')\mathbf{x} = 0$ corresponds to the eigenmode $|\Psi\rangle = x_1|\sigma,m\rangle + x_2|\sigma',m'\rangle$. Near the intersection point $[q_0,\bar{\beta}_m(q_0)]$ by introducing the following detunings,

$$\kappa = \beta - \bar{\beta}_m(q_0), \quad \varepsilon = q - q_0, \tag{16}$$

one can linearize the eigenvector equation $G(m,m')\mathbf{x} = 0$:

$$\begin{pmatrix} J\varepsilon - \kappa & Q \\ Q & J'\varepsilon - \kappa \end{pmatrix}\mathbf{x} = 0. \tag{17}$$

The spectra of coupled modes are obtained in the form

$$\beta = \bar{\beta}_m(q_0) + \tfrac{1}{2}[\varepsilon(J + J') \pm 2\Gamma], \tag{18}$$

where $\Gamma = \frac{1}{2}\sqrt{(\varepsilon M)^2 + 4Q^2}$; $M = J' - J$. Equation (18) describes the known effect of repulsion of the spectral curves [1]. The expressions for such hybridized modes read as (in the laboratory frame)

$$\begin{aligned} |\psi_1\rangle &= \left\{C_1|\sigma,m\rangle \exp\left[i\left(\tilde{\beta}_m + \frac{\varepsilon}{2}M\right)z\right]\right. \\ &\quad \left. + C_2|\sigma',m'\rangle \exp\left[i\left(\tilde{\beta}_{m'} - \frac{\varepsilon}{2}M\right)z\right]\right\}\exp(iz\Gamma), \\ |\psi_2\rangle &= \left\{C_2|\sigma,m\rangle \exp\left[i\left(\tilde{\beta}_m + \frac{\varepsilon}{2}M\right)z\right]\right. \\ &\quad \left. - C_1|\sigma',m'\rangle \exp\left[i\left(\tilde{\beta}_{m'} - \frac{\varepsilon}{2}M\right)z\right]\right\}\exp(-iz\Gamma), \end{aligned} \tag{19}$$

where $C_{1,2} = \frac{1}{\sqrt{2}}\sqrt{1 \mp \frac{\varepsilon M}{2\Gamma}}$, so that $|C_1|^2 + |C_2|^2 = 1$.

As usual, mode coupling implies intermodal transitions between zero-approximation fields. Indeed, if a semi-infinite MHF is excited with the OV $|\sigma,m\rangle$, in the simplest reflectionless approximation the field within the fiber is described by

$$\begin{aligned} |\Phi\rangle &= |\sigma,m\rangle \exp[i(\tilde{\beta}_m - \tilde{\beta}_{m'} + \varepsilon M)z]\left(\cos\Gamma z - i\frac{\varepsilon M}{2\Gamma}\sin\Gamma z\right) \\ &\quad + \frac{iQ}{2\Gamma}\sin\Gamma z|\sigma',m'\rangle. \end{aligned} \tag{20}$$

At zero detuning $\varepsilon = 0$ the evolution of the field has the simplest form and yields the total conversion of the OV $|\sigma,m\rangle$ into the OV $|\sigma',m'\rangle$ at the conversion length $s_k = \pi(2k + 1)/2Q$, $k = 0,1,2\cdots$. Equations (18)–(20) generalize the earlier obtained results of Refs. [1–3]. It should be noted that the conversion length depends on the conversion type only through the coupling constant Q. As has been mentioned previously, each part of the perturbation operator $\hat{V}$ is responsible for a special kind of mode conversion.

Since the effect of the scalar-type perturbation described by the $k^2\nu^2$ term has been exhaustively studied in earlier papers [1–4], we focus our attention on the transitions enabled by the SOI term $\hat{V}_{\rm so}$. The corresponding coupling constant for the transition $|\sigma,m\rangle \to |\sigma',m'\rangle$, where selection rules [Eq. (12)] are justified, can be brought to the form

$$\begin{aligned} Q = K\int_0^\infty \left\{ RF_m''F_m' + RF_m'F_{m'}' \right. \\ + F_m'F_{m'}[1 - \sigma(m \pm \ell)] - (2m\sigma + 1)F_m' \\ \left. - mF_m\left(\sigma F_{m'}' \mp \frac{\ell}{R}F_{m'}\right)\right\}\frac{\partial f}{\partial R}dR, \end{aligned} \tag{21}$$

where $K = \frac{\Delta\delta}{2kr_0^2 n_{\rm co}\sqrt{N_m N_{m'}}}$, $R = r/r_0$, r_0 is the core's radius, and the normalization coefficient is $N_m = \int_0^\infty RF_m^2 dR$. It is assumed here that Q is defined by Eq. (15). In the following we restrict our considerations to the case of step-index fibers, where $\frac{\partial f}{\partial R} = \delta(R - 1)$; $\delta(x)$ is the Dirac function [30]. Since also $F_m(R = 1) = 1$ one can simplify Eq. (21) and bring it to

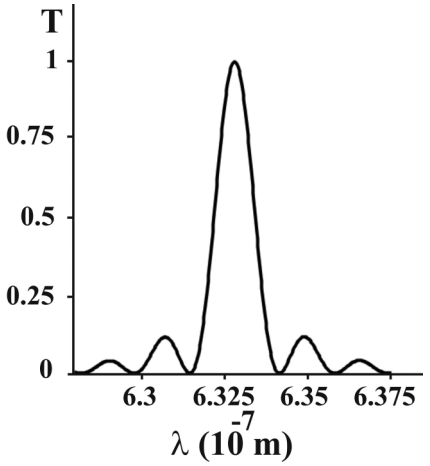

FIG. 3. Transmission coefficient T plotted in the reflectionless approximation for the SOI-induced conversion of the OV $|1,1\rangle$ into the OV $|-1,5\rangle$ in an elliptical spun fiber ($\ell = 2$). Fiber parameters: $n_{co} = 1.5$, $\Delta = 10^{-2}$, $\delta = 5 \times 10^{-2}$, $r_0 = 10\lambda_0$, $\lambda_0 = 6.328 \times 10^{-7}$ m.

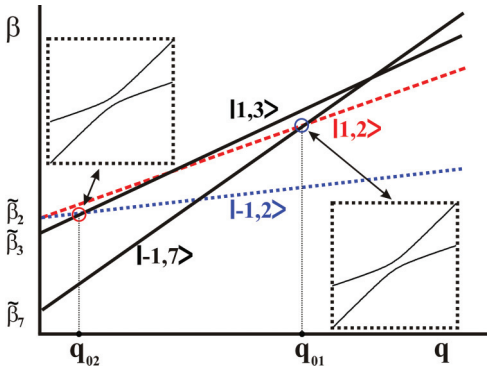

FIG. 4. (Color online) Controlling the OAM state of the outcoming beam by controlling the polarization state of the input field. By changing the circular polarization of the input OV with the topological charge 2 from right (red dashed line $|1,2\rangle$) to left (blue dotted line $|-1,2\rangle$) one can generate OVs of either charge 7 or 3 (black solid labeled lines). The SOI-induced conversion $|1,2\rangle \to |-1,7\rangle$ ($M = +3$) occurs at q_{01}, whereas the transformation process $|-1,2\rangle \to |1,3\rangle$ ($M = +3$) takes place at q_{02} (here $\ell = 3$). Insets show repulsion of spectral curves due to mode coupling [see also Eq. (18)].

the form

$$Q = K\{F_m'' F_m' + F_m' F_{m'}' - \sigma(3m \pm \ell)F_m' - m(\sigma F_{m'}' \mp \ell)\}_{R=1}. \quad (22)$$

Note that here the derivatives should be taken with respect to R and F_m depends on $\tilde{U}R$, where $\tilde{U}$ is the known fiber parameter [30]. Figure 3 shows a typical transmittance curve plotted in the reflectionless approximation for the SOI-induced conversion of the OV $|1,1\rangle$ into the OV $|-1,5\rangle$ in an elliptical spun fiber ($\ell = 2$). Note that here it is the term $\delta\hat{H}_{so}$ which enables this conversion.

Among the perturbation terms the SOI operator $\hat{V}_{so}$ provides the weakest coupling. Indeed, using the definition of $\Phi(r)$ Eq. (1) one can show that the matrix elements with this operator are proportional to $(\hat{V}_{SO})_{ij} \propto \Delta\delta/r_0^2$, since the scale of spatial variations of the functions $F_m(r)$ has the order of core's radius. The scalar-perturbation term generates the matrix elements of order $(k^2\nu^2)_{ij} \propto \Delta\delta k^2$, which is clear from its definition. The case where such elements are the largest will be further referred to as the case of a strongly perturbed fiber. The order of the matrix elements generated by the ideal-fiber SOI operator $\hat{H}_{so}$ can be assessed as $(\hat{H}_{SO})_{ij} \propto \Delta/r_0^2$. Once again, this estimate is based on the fact that upon transition to the dimensionless variable R the expression [Eq. (5)] acquires a general multiplier of r_0^{-2}. This set of matrix elements can also be the largest among the three sets of perturbation matrix elements; the corresponding condition reads as $\delta \ll (\lambda/r_0)^2$, where λ is the wavelength (see also [31]). This hierarchy of interactions, as will be shown further, is essential for implementation of certain transitions not forbidden by the selection rules.

Unlike the transitions induced by the scalar-type perturbation term $k^2\nu^2$, the SOI-induced transitions, governed by the selection rules [Eq. (12)], make principally possible the control of the OAM state of the outcoming beam by controlling the polarization state of the input field. Indeed, in an $\ell = 3$ MHF along with the SOI-induced conversion $|1,2\rangle \to |-1,7\rangle$ ($M = +3$), the transformation process $|-1,2\rangle \to |1,3\rangle$ ($M = +3$) is also possible. This example shows that by changing the circular polarization of the input OV with the topological charge 2 from right to left one can generate OVs of either charge 7 or 3. In this way, such a control is formally possible. However, these resonance transitions occur at different values of q (see Fig. 4): The first one takes place in the lattice with $q_{01} = (\tilde{\beta}_2 - \tilde{\beta}_7)/3$, whereas the second transition requires the lattice with $q_{02} = (\tilde{\beta}_2 - \tilde{\beta}_3)/3$. Moreover, since calculations of the coupling integrals [Eqs. (21) and (22)] in these cases imply integrations of the products of radial functions with orbital indices $l = 2,7$ and $l = 2,3$, respectively, the conversion lengths would also be different. So, the conversion process $|1,2\rangle \to |-1,7\rangle$ occurs at the resonance pitch 2×10^{-4} m and is accomplished at the conversion length $s_0 = 2.6 \times 10^{-2}$ m (fiber parameters are given in the legend for Fig. 3). On the contrary, the conversion $|-1,2\rangle \to |1,3\rangle$ requires resonance pitch of $H = 2 \times 10^{-3}$ m and the conversion length is $s_0 = 7.5 \times 10^{-2}$ m. That is why it is hardly possible to implement spin control over the OAM state through such devices.

All the above-studied cases were related to intersections of nondegenerate spectral curves. Consider now resonance points formed by intersections of spectral curves with a double-degenerate $J = 0$ spectral curve, which corresponds to $|1,-1\rangle$ and $|-1,1\rangle$ OVs [see Fig. 2(b)]. To allow for the effect of the standard ideal-fiber SOI described by the term $\hat{H}_{so}$ one has to construct the perturbation matrix in the space spanned over the states $|1,-1\rangle$, $|-1,1\rangle$. Since the scalar propagation constants for such scalar-approximation modes coincide and $J = J' = 0$ the perturbation matrix equation (14) reduces to the form

$$G(1,1) = \begin{pmatrix} \tilde{\beta}_1^2 - \beta^2 + 2\tilde{\beta}_0 b_1 & 2\tilde{\beta}_0 b_1 \\ 2\tilde{\beta}_0 b_1 & \tilde{\beta}_1^2 - \beta^2 + 2\tilde{\beta}_0 b_1 \end{pmatrix}, \quad (23)$$

where $b_1 = \langle 1,-1|\hat{H}_{so}|-1,1\rangle/2\tilde{\beta}_0$ is the ideal-fiber SOI constant [31]. It should be stressed that in this particular case $m = m' = 1$ and $\hat{H}_{so}$ also gives a contribution to the diagonal elements of this matrix. At $m \neq m'$ such elements either do not appear or are irrelevant. In like manner, the eigenvalue equation $G(1,1)\mathbf{x} = 0$ can be brought to the form analogous to Eq. (17):

$$\begin{pmatrix} -\kappa + b_1 & b_1 \\ b_1 & -\kappa + b_1 \end{pmatrix} \mathbf{x} = 0, \tag{24}$$

where $\kappa = \beta - \tilde{\beta}_1$. Analogously, the solution $\mathbf{x} = \mathrm{col}(x_1,x_2)$ corresponds to the eigenmode $|\Psi\rangle = x_1|1,-1\rangle + x_2|-1,1\rangle$. One readily obtains from this equation the splitting of spectrum curves:

$$\beta_1 \equiv \beta_{TM} = \tilde{\beta}_1 + 2b_1, \quad \beta_2 \equiv \beta_{TE} = \tilde{\beta}_1. \tag{25}$$

The eigenvector $\mathbf{x}_1 = \mathrm{col}(1,1)$, which corresponds to β_1, represents the mode $|\mathrm{TM}\rangle = |1,-1\rangle + |-1,1\rangle$, whereas the eigenvector $\mathbf{x}_2 = \mathrm{col}(1,-1)$ belongs to the eigenvalue β_2 and represents the TE mode: $|\mathrm{TE}\rangle = |1,-1\rangle - |-1,1\rangle$ [31]. As is evident, since for weakly guiding fibers one has $\tilde{\beta}_i \approx kn_{co}$ [30], the distance between these split spectrum curves has the order of Δ/kr_0^2 and is proportional to the SOI coupling.

Consider now intersection of $|\mathrm{TE}\rangle$ and $|\mathrm{TM}\rangle$ spectral curves with some other spectral curve that corresponds to a mode $|\sigma_\alpha,l_\alpha\rangle$. Using Eq. (7) one can easily determine that this curve intersects with the $|\mathrm{TE}\rangle$ and $|\mathrm{TM}\rangle$ curves at $q_{TE} = (\beta_{TE} - \tilde{\beta}_\alpha)/J$ and $q_{TM} = (\beta_{TM} - \tilde{\beta}_\alpha)/J$, where $J = \sigma_\alpha + l_\alpha$. From Eq. (25) the separation of these points in the q domain is

$$\eta \equiv q_{TM} - q_{TE} = 2b_1/J \propto \Delta/kr_0^2. \tag{26}$$

As is obvious, this quantity has also the order of separation of the spectral curves for the TE and TM modes. On the other hand, as follows from Eqs. (18) and (19), in the q domain the width of the coupling area is proportional to the coupling constant Q. The order of this parameter is determined by the order of the perturbation term, which is responsible for the corresponding resonance mode coupling. In this way, the width of the resonance area for coupling mediated by the SOI operator $\hat{V}_{so}$ has the order of $\Delta\delta/kr_0^2$, whereas the width of the area, where the coupling mediated by the scalar-perturbation term $k^2\nu^2$ is essential, has the order of $\Delta\delta k$. These estimates are critical for understanding the nature of mode coupling in such a nearly degenerate regime.

Indeed, if the coupling with $J = 0$ TE and TM modes, whose spectral curves are closely spaced, is caused by the weakest $\hat{V}_{so}$ perturbation term, the distance between the intersection points η is much greater than the width $\Delta\delta/kr_0^2$ of the resonance area, where the coupling is still essential: $\eta = \Delta/kr_0^2 \gg \Delta\delta/kr_0^2$ [see Fig. 5(a)]. In this situation there is no cross influence of resonance transitions between the mode $|\alpha\rangle$ and the $|\mathrm{TE}\rangle$ and $|\mathrm{TM}\rangle$ modes. In each of the points one has the standard case of the two-mode coupling and the mode conversion in such well-separated points will run between the input excited mode $|\alpha\rangle$ and the $|\mathrm{TE}\rangle$ (or $|\mathrm{TM}\rangle$, depending on the resonance point) mode. Note that if $|\alpha\rangle$ can be coupled to the $|\mathrm{TE}\rangle$ mode it also can be coupled with the $|\mathrm{TM}\rangle$ mode. Exactly this possibility is reflected in Table 3 of Ref. [14]. Naturally, such a coupling between the input field $|\alpha\rangle$ and $|\mathrm{TE}\rangle$, $|\mathrm{TM}\rangle$ modes can also be mediated by the scalar-perturbation term $k^2\nu^2$. In this case the situation will be qualitatively the same only for weakly perturbed MHFs, that is, the fibers in which the influence of the standard SOI term $\hat{H}_{so}$ is much greater than the influence of the scalar perturbation [this takes place at $\delta \ll (\lambda/r_0)^2$]. All the above-mentioned cases enable generation of radially and azimuthally polarized beams, which is a topical problem in modern optics [36].

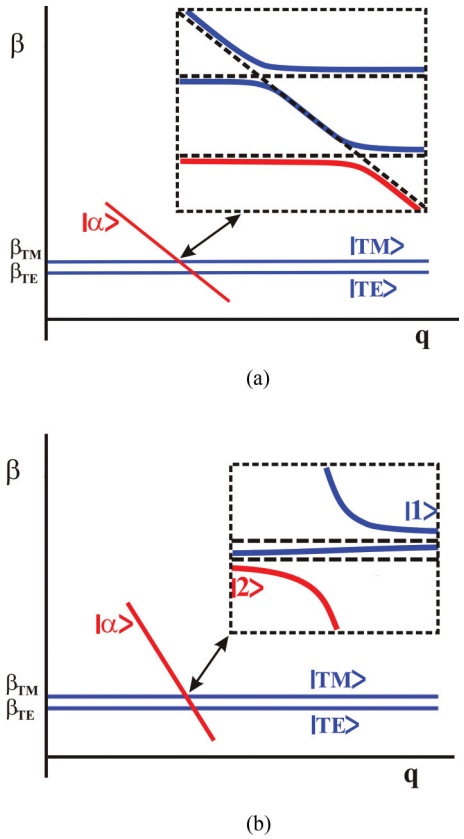

FIG. 5. (Color online) Hybridization of spectral curves with nearly degenerate $J = 0$ curves. For the case where the width of the coupling area is much less than the distance between the $|\mathrm{TE}\rangle$ and $|\mathrm{TM}\rangle$ spectral curves (a) the two-mode coupling scheme is implemented and the transitions in such well-separated points run between the corresponding input mode $|\alpha\rangle$ (red line) and the $|\mathrm{TE}\rangle$ or $|\mathrm{TM}\rangle$ modes (blue lines) leading to transformation of spectral curves (see inset). In the opposite case (b) the mode coupling affects the input mode $|\alpha\rangle$ and one of the OVs $|1,-1\rangle$, $|-1,1\rangle$, which form the hybrid modes with the spectral curves $|1\rangle$ and $|2\rangle$ (see inset). The remaining OV of the pair $|1,-1\rangle$, $|-1,1\rangle$ is uncoupled and its spectral curve (middle blue line in inset) does not hybridize.

However, the situation will be drastically different if the transition-enabling scalar perturbation is much greater than the standard SOI, which takes place at $\delta \gg (\lambda/r_0)^2$. In this case the separation of the resonance points in the q domain is insufficient to prevent the effective cross influence between the neighboring hybridized spectral curves, which essentially overlap. To establish the type of coupling one has to build the perturbation matrix G over the *three* states in question [37]. Since the scalar perturbation $k^2\nu^2$ couples the states according to selection rules Eq. (11), that is, regardless of their spin states,

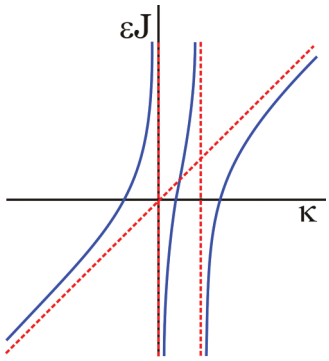

FIG. 6. (Color online) Schematic plot of the spectral curves in the intermediate case of comparable coupling constants Q, b_1 in Eq. (29).

the eigenvalue equation in the three-component vector $\mathbf{x}_3$ can be represented near the intersection region as

$$\begin{pmatrix} J\varepsilon-\kappa & Q & 0 \\ Q & b_1-\kappa & b_1 \\ 0 & b_1 & b_1-\kappa \end{pmatrix}\mathbf{x}_3 = 0. \tag{27}$$

Here for definiteness we have assumed without the loss of generality $|\alpha\rangle = |1,l_\alpha\rangle$, so that the vector $\mathbf{x}_3$ stands for the field $|\Psi\rangle = x_1|\alpha\rangle + x_2|1,-1\rangle + x_3|-1,1\rangle$. Note that in this case $b_1 \ll Q$ and Eq. (27) can be decomposed into two eigenvalue equations:

$$\begin{pmatrix} J\varepsilon-\kappa & Q \\ Q & b_1-\kappa \end{pmatrix}\mathbf{x}_2 = 0, \quad (b_1-\kappa)\mathbf{x}_1 = 0, \tag{28}$$

where $\mathbf{x}_2$ belongs to the space spanned over $\{|\alpha\rangle,|1,-1\rangle\}$ states and a one-dimensional vector $\mathbf{x}_1$ is related to the field $|-1,1\rangle$. The first of these equations, obviously, describes the coupling between the fields $|\alpha\rangle$ and $|1,-1\rangle$. The second equation conveys the fact that the second OV $|-1,1\rangle$ remains uncoupled and its spectral curve does not change. The behavior of the spectral curves in this case is shown in Fig. 5(b).

This result can be understood in the following manner. Being in this case the strongest interaction, the scalar perturbation first couples the two fields $\{|\alpha\rangle,|1,-1\rangle\}$, which satisfy the selection rule, Eq. (11), forming a typical two-mode hybrid spectral curve. Then the relatively small standard SOI term couples the remaining OV $|-1,1\rangle$ to the newly formed hybrid modes. However, since this coupling is weak, the resulting field will be approximately the same as after the first coupling in this "succession" of couplings. In the intermediate case of comparable constants Q, b_1 it is possible to plot the spectral curves, which on the plane $(\kappa,\varepsilon J)$ satisfy the equation

$$\varepsilon J = \kappa - \frac{Q^2(\kappa-b_1)}{\kappa(\kappa-2b_1)}. \tag{29}$$

The plot of this curve is given in Fig. 6. As is evident, in the limit $b_1 \ll Q$ the central curve tends to the straight line, and the whole plot turns into the one presented in the inset in Fig. 5(b).

Summarizing, one can say that in the case of strong scalar perturbation neither $|\mathrm{TE}\rangle$ nor $|\mathrm{TM}\rangle$ modes can be formed in the process of resonance mode generation in MHFs. Instead, this coupling process leads to generation of either $|1,-1\rangle$ or $|-1,1\rangle$ OVs. This contradicts the corresponding statement of Ref. [14], according to which the only possible type of $J=0$ mode generation is the generation of $|\mathrm{TE}\rangle$ and $|\mathrm{TM}\rangle$ modes. Moreover, the fiber parameters used there in numerical simulations are related rather to the case of strong ellipticity, where the scalar perturbation is the strongest interaction and only the fields $|1,-1\rangle$ and $|-1,1\rangle$ can be generated in the points of intersection with the degenerate spectrum lines.

Finally, let us discuss the possibility of implementing such processes of mode conversion in waveguides designed for other spectral ranges. Although for state-of-the-art technology manufacturing long-period chiral fiber gratings for optical range is no longer a challenge, making laboratory experiments on verification of the suggested theory using other types of dielectric waveguides may prove to be convenient. This technique of modeling the optical processes in a different wavelength range is rather widely used by experimentalists and is very fruitful (see, for example, Refs. [23,38]). To assess applicability of our results to other wavelength ranges it is necessary to study the scaling properties of the main relations, which the physics of mode conversion is based on. The main question here is how the waveguide should be scaled to possess the same transformation properties for a different wavelength range. Even a superficial analysis reveals the essential difference in this relation between MHFs and planar chiral structures, such as, for example, cholesteric liquid crystals. Indeed, in cholestericlike systems the transmittance can be described in terms of a dimensionless combination "λ/H," for example. In this way, the transmittance properties for a lattice with a larger pitch are the same provided the central wavelength λ_0, at which the conversion is maximally effective, is properly scaled.

In MHFs such a simple scaling is insufficient since there is an extra dimension parameter, namely, the fiber's radius, which also determines the properties of the system, such as its waveguide parameter V [30], the coupling integral K [Eq. (21)], etc. By keeping intact only the ratio of λ/H, as proves to be sufficient for cholesterics, one would obtain, for example, the distortion of Figs. 2(a) and 4. This distortion takes place because the scalar propagation constants $\tilde{\beta}_m$, which determine vertical displacements of the spectral curves, depend on the core's radius. In this way, one cannot establish the value of the resonance lattice pitch for any wavelength knowing only such a pitch value for a certain wavelength.

To establish necessary scale transformations, which one has to make over the system to keep invariant the results obtained for a certain spectral range, consider dimensionless forms of the basic relations for mode conversion. Using a well-known relation [30],

$$\tilde{\beta}_m = \frac{1}{r_0}\sqrt{\frac{V^2}{2\Delta} - \tilde{U}_m^2} \equiv \frac{n_m}{r_0}, \tag{30}$$

where $V = 2\pi\frac{\lambda}{r_0}n_{\mathrm{co}}\sqrt{2\Delta}$ and $\tilde{U}_m$ is determined through V from the known dimensionless characteristic equation, one can bring the kinematical resonance condition, Eq. (9), to a dimensionless form,

$$\frac{r_0}{H_0} = \frac{n_{m'} - n_m}{J - J'}, \tag{31}$$

where H_0 is the resonance pitch. Note that n_m depends on the dimensionless parameter $\xi = \lambda/r_0$. As is evident from this relation and the definition of V, the kinematical resonance condition, Eq. (31), is invariant under a simultaneous scaling:

$$\lambda \to \gamma\lambda, \quad r_0 \to \gamma r_0, \quad H_0 \to \gamma H_0. \tag{32}$$

This implies that in a MHF with the pitch γ times greater than that of a certain etalon MHF the corresponding mode conversion would take place at the γ times greater resonance wavelength, provided the core's radius is γ times increased.

In like manner one can show that under the scaling transformation, Eq. (32), the form of the transmittance curve (see Fig. 3) would also be maintained. To prove this it is useful to notice that the coupling constant Q [Eq. (21)] can be represented as $Q = \bar{Q}(\xi)/r_0$, where $\bar{Q}$ is the dimensionless function. Then Eq. (19) for coupled modes can be recast in terms of dimensionless variables $\zeta = z/r_0$ and $\bar{\varepsilon} = \varepsilon r_0$ by changing $\tilde{\beta}_m \to n_m$; for example,

$$|\psi_1\rangle = \left\{ C_1|\sigma,m\rangle \exp\left[i\left(n_m + \frac{\bar{\varepsilon}}{2}M \right)\zeta \right] + C_2|\sigma',m'\rangle \exp\left[i\left(n_{m'} - \frac{\bar{\varepsilon}}{2}M \right)\zeta \right] \right\} \exp(i\zeta\bar{\Gamma}), \tag{33}$$

where $\bar{\Gamma} = \Gamma r_0$. Under the scale transformation equation (32) this implies that the width of the resonance area (in the q domain) decreases γ times, which entails increasing of the width of the transmittance curves in the λ domain by the same factor. Analogously, the conversion length s_k also increases γ times.

V. CONCLUSION

In the present paper we have studied the effect of the spin-orbit interaction on generation and conversion of optical vortices in multihelicoidal fibers. On the basis of a consistent analytical approach we have obtained an effective translation-invariant vector wave equation for this problem. By applying degenerate perturbation theory we have obtained the spectra of resonant coupled modes and their structure. We have shown that if the obtained selection rules are justified, in this system a SOI mediated conversion of optical vortices into vortices with changed topological charge is possible in a narrow spectral range. The charges of the generated vortices are found to differ from the charge of the input vortex by $\pm(\ell \pm 2)$, where ℓ is the number of helical branches in the refractive index distribution of the fiber. We have also shown that the spin-orbit interaction may lead to a narrow-band generation of radially and azimuthally polarized TE and TM modes from certain optical vortices. Such generation caused by the scalar-type multihelicoidal perturbation of form is possible only for weakly deformed fibers, whereas for strongly deformed fibers such perturbation may result only in generation of vortices with zero total angular momentum. We have studied the possibility of polarization control over the orbital angular momentum of the generated state in such a system and found it impossible for a MHF with nonvarying parameters.

ACKNOWLEDGMENTS

The authors are grateful to the reviewer for bringing to their attention the question of scaling properties of MHFs. C.N.A., B.P.L., and M.A.Y. acknowledge support of the state grant of Ukraine, Grant No. GP/F49/113.

[1] C. N. Alexeyev and M. A. Yavorsky, Phys. Rev. A **78**, 043828 (2008).
[2] C. N. Alexeyev, T. A. Fadeyeva, B. P. Lapin, and M. A. Yavorsky, Phys. Rev. A **83**, 063820 (2011).
[3] C. N. Alexeyev, Appl. Opt. **51**, 6125 (2012).
[4] C. N. Alexeyev, B. P. Lapin, A. V. Volyar, and M. A. Yavorsky, Opt. Lett. **38**, 2277 (2013); C. N. Alexeyev, Y. A. Fridman, B. P. Lapin, and M. A. Yavorsky, J. Opt. **15**, 125401 (2013).
[5] C. N. Alexeyev, Appl. Opt. **52**, 433 (2013).
[6] X. M. Xi, T. Weiss, G. K. L. Wong, F. Biancalana, S. M. Barnett, M. J. Padgett, and P. S. J. Russell, Phys. Rev. Lett. **110**, 143903 (2013).
[7] J. Wang, J.-Y. Yang, I. M. Fazal, N. Ahmed, Y. Yan, H. Huang, Y. Ren, Y. Yue, S. Dolinar, M. Tur, and A. E. Willner, Nat. Photon. **6**, 488 (2012).
[8] L. Veissier, A. Nicolas, L. Giner, D. Maxein, A. S. Sheremet, E. Giacobino, and J. Laurat, Opt. Lett. **38**, 712 (2013).
[9] D. Zhang, X. Feng, and Y. Huang, Opt. Express **20**, 26986 (2012).
[10] Y. Zhang, I. B. Djordjevic, and X. Gao, Opt. Lett. **37**, 3267 (2012).
[11] N. Bozinovic, Y. Yue, Y. Ren, M. Tur, P. Kristensen, H. Huang, A. E. Willner, and S. Ramachandran, Science **340**, 1545 (2013).
[12] P. Boffi, P. Martelli, A. Gatto, and M. Martinelli, J. Opt. **15**, 075403 (2013).
[13] H. Xu, L. Yang, Z. Han, and J. Qian, Opt. Commun. **291**, 207 (2013).
[14] H. Xu and L. Yang, Opt. Lett. **38**, 1978 (2013).
[15] L. Yang, L.-L. Xue, C. Li, J. Su, and J.-R. Qian, Opt. Express **19**, 2251 (2011).
[16] L. Yang, L. Xue, J. Su, and J. Qian, Chin. Opt. Lett. **9**, 070603 (2011).
[17] R. D. Birch, Electron. Lett. **23**, 50 (1987).
[18] C. D. Poole, C. D. Townsend, and K. T. Nelson, J. Lightwave Technol. **9**, 598 (1991).
[19] K. S. Lee and T. Erdogan, J. Opt. Soc. Am. A. **18**, 1176 (2001).
[20] V. I. Kopp and A. Z. Genack, Nat. Photonics **5**, 470 (2011).
[21] V. I. Kopp, V. M. Churikov, J. Singer, N. Chao, D. Neugroschl, and A. Z. Genack, Science **305**, 74 (2004).
[22] G. Shvets, S. Trendafiliv, V. I. Kopp, D. Neugroschl, and A. Z. Genack, J. Opt. A: Pure Appl. Opt. **11**, 074007 (2009).
[23] V. I. Kopp and A. Z. Genack, Opt. Lett. **28**, 1876 (2003).
[24] V. I. Kopp, V. M. Churikov, and A. Z. Genack, Opt. Lett. **31**, 571 (2006).

[25] V. I. Kopp, V. M. Churikov, G. Zhang, J. Singer, C. W. Draper, N. Chao, D. Neugroschl, and A. Z. Genack, J. Opt. Soc. Am. B **24**, A48 (2007).

[26] T. Weiss, G. K. L. Wong, F. Biancalana, S. M. Barnett, X. M. Xi, and P. St. J. Russell, J. Opt. Soc. Am. B **30**, 2921 (2013).

[27] R. B. Shang, W. G. Zhang, W. B. Zhu, P. C. Geng, J. Ruan, S. C. Gao, X. N. Li, Q. X. Cao, and X. Zeng, J. Opt. **15**, 075402 (2013).

[28] Y. V. Kartashov, V. A. Vysloukh, and L. Torner, Opt. Lett. **38**, 3414 (2013).

[29] C. N. Alexeyev, A. V. Volyar, and M. A. Yavorsky, J. Opt. A: Pure Appl. Opt. **9**, 537 (2007).

[30] A. W. Snyder and J. D. Love, *Optical Waveguide Theory* (Chapman and Hall, London, New York, 1985).

[31] C. N. Alexeyev, A. V. Volyar, and M. A. Yavorsky, in *Lasers, Optics and Electro-Optics Research Trends*, edited by L. I. Chen (Nova Publishers, New York, 2007), pp. 131–223.

[32] V. S. Liberman and B. Ya. Zel'dovich, Phys. Rev. A **46**, 5199 (1992).

[33] A. V. Dooghin, N. D. Kundikova, V. S. Liberman, and B. Y. Zel'dovich, Phys. Rev. A **45**, 8204 (1992).

[34] K. Yu. Bliokh and Yu. P. Bliokh, Phys. Lett. A **333**, 181 (2004).

[35] *Twisted Photons: Applications of Light with Orbital Angular Momentum*, edited by J. P. Torres and L. Torner (Wiley-VCH Verlag GmbH & Co. KGaA, Weinheim, 2011).

[36] E. V. Barshak, C. N. Alexeyev, and M. A. Yavorsky, J. Opt. **15**, 125707 (2013); H. I. Sztul, D. A. Nolan, G. Milione, X. Chen, J. Koh, and R. R. Alfano, Proc. SPIE **7227**, 722704 (2009); G. Milione, H. I. Sztul, and R. R. Alfano, *ibid.* **7613**, 761305 (2010); G. Milione, H. I. Sztul, D. A. Nolan, J. Kim, M. Etienne, J. McCarthy, J. Wang, and R. R. Alfano, *ibid.* **7950**, 79500K (2011); C. N. Alexeyev, E. V. Barshak, T. A. Fadeyeva, A. V. Volyar, and M. A. Yavorsky, J. Opt. **13**, 075706 (2011).

[37] C. N. Alexeyev and M. A. Yavorsky, J. Opt. A: Pure Appl. Opt. **10**, 085006 (2008).

[38] V. I. Kopp and A. Z. Genack, Phys. Rev. Lett. **89**, 033901 (2002); V. I. Kopp, R. Bose, and A. Z. Genack, Opt. Lett. **28**, 349 (2003).